Evolutionary rescue during extreme drought

Daniel N. Anstett[1-5,*], Julia Anstett[6,7], Seema N. Sheth[8], Dylan R. Moxley[5,9], Mojtaba Jahani[5], Kaichi Huang[5], Marco Todesco[5,9,10], Rebecca Jordan[11], Jose Miguel Lazaro-Guevara[5,12,13], Loren H. Rieseberg[5], Amy L. Angert[5,14]

[1] School of Integrative Plant Science, Section of Biology and the L. H. Bailey Hortorium, Cornell University, Ithaca, NY 14853, USA
[2] Plant Resilience Institute, Michigan State University, East Lansing, MI 48824, USA
[3] Department of Plant Biology, Michigan State University, East Lansing, MI 48824, USA
[4] Department of Entomology, Michigan State University, East Lansing, MI 48824, USA
[5] Biodiversity Research Centre and Department of Botany, University of British Columbia, Vancouver, BC V6T 1Z4, Canada
[6] Genomic Sciences and Technology Program, University of British Columbia, Vancouver, British Columbia, V6T 1Z4, Canada
[7] Department of Microbiology and Immunology, University of British Columbia, Vancouver, British Columbia, V6T 1Z4, Canada
[8] Department of Plant and Microbial Biology, North Carolina State University, Raleigh, NC, USA
[9] Michael Smith Laboratories, University of British Columbia, Vancouver, British Columbia V6T 1Z4, Canada
[10] Department of Biology, University of British Columbia, Kelowna, British Columbia V1V 1V7, Canada
[11] CSIRO Environment, Sandy Bay, Tasmania 7005, Australia
[12] Division of Medical Genetics, Department of Medicine, McGill University Health Centre (MUHC), Montreal, QC, H3G 2M1, Canada
[13] Department of Human Genetics, McGill University, Montreal, QC, H3A 0C7, Canada
[14] Department of Zoology, University of British Columbia, Vancouver, British Columbia V6T 1Z4, Canada
* Corresponding author, dna38@cornell.edu

Abstract

Populations declining due to climate change may need to evolve to persist. While evolutionary rescue has been demonstrated in theory and the lab, its relevance to natural populations facing climate change remains unknown. Here we link rapid evolution and population dynamics in scarlet monkeyflower, *Mimulus cardinalis*, during an exceptional drought. We leverage whole-genome sequencing across 55 populations to identify climate-associated loci. Simultaneously we track demography and allele frequency change throughout the drought. We establish range-wide population decline during the drought, geographically variable rapid evolution, and variable population recovery that is predictable by both standing genetic variation and rapid evolution at climate-associated loci. These findings demonstrate evolutionary rescue in the wild, showing that genomic variability at adaptive, but not neutral loci, predicts population recovery.

Main Text

Climate change is leading to population declines due to increasing severity and duration of extreme events (*1-3*). Reversing such declines may depend on evolutionary rescue, where evolution over a small number of generations leads to demographic recovery (*4*). Evolutionary rescue has extensive theoretical support (*5, 6*) and elegant lab demonstrations in microorganisms (*7-9*), but definitive demonstrations in wild populations in response to climate change have been elusive. The best evidence for evolutionary rescue outside the lab is herbicide resistance in response to modern agriculture (*10, 11*), transmissible cancer resistance in Tasmanian devils (*12*), and adaptation to pollution in killifish (*13*). However, these studies represent situations with incredibly strong selection from a single novel stressor, so it remains unclear whether they are good analogs for the multivariate, non-linear, and cyclical events associated with climate change. Additionally, these studies have indirect linkages between shifts in allele frequency and population demography. Documenting evolutionary rescue in the wild requires demonstrating (1) demographic decline driven by an environmental perturbation, (2) rapid evolution during population decline, and (3) demographic recovery that results from evolutionary change (Fig. 1A).

We demonstrate evolutionary rescue during an exceptional drought in a riparian plant, scarlet monkeyflower (*Mimulus cardinalis*), by leveraging extensive demographic and landscape genomics datasets. *Mimulus cardinalis* is a perennial herb present in lowland and mountainous habitats from northern Baja California, Mexico through southern Oregon, USA. Much of the species' range has been impacted by a 22-year megadrought (*14*), with the 2012-2015 drought representing the most extreme four-year drought in more than 10,000 years in California (*15*). The frequency of these "exceptional" drought events is projected to increase with climate change (*2, 16*) increasing the vulnerability of California and many other Mediterranean-type ecosystems to drought stress. Since *M. cardinalis* occurs along an aridity gradient, and has geographic variability in adaptation to this aridity (*17, 18*), the species is an ideal system to study geographical variation in drought adaptation over space and time.

We first assessed the impact of drought on *M. cardinalis* population dynamics. Through annual field surveys from 2010 to 2018, we collected demographic data on survival, growth, reproduction, and recruitment from 19 populations along a North-South transect encompassing most of the range of *M. cardinalis* (Fig. 2B). We used these data to infer population growth rate ($\boldsymbol{\lambda}$) through integral projection modeling (IPM) (Fig. 1B; Supplementary Methods) (*19*). Fifteen populations were projected to decline from the beginning to the end of the extreme drought (Fig. 1C-D; Fig. S1). Lower winter precipitation was the best predictor of lower mean population growth rate during the drought (Fig. 1E; Table S1), further implicating drought stress as a likely cause of these population declines.

Having established demographic decline during the exceptional drought, we then leveraged an extensive spatiotemporal collection of seed and leaf tissue to (a) identify single nucleotide polymorphisms (SNPs) associated with historical climate and (b) track their evolution during the contemporary drought (Fig. 2). First, we identified SNPs associated with 30-year pre-drought climate averages (1981-2010) by sequencing a "baseline" dataset of 55 populations (Fig. 2B). These populations were sampled across the entire range of *M. cardinalis* from 2007 to 2011, a baseline time period just prior to the exceptional 2012-2015 drought (Fig. 1C, Table S2). The

baseline dataset is composed of whole-genome sequences of 347 individuals at 6 to 21X coverage, identifying a total of 2,156,443 SNPs. We combined SNP-based (*20*) and window-based (*21*) Genotype-Environment Associations (GEAs) to identify SNPs with strong association with the historical climate (Fig. 2C). To perform these analyses, we used 9 climate variables (*22*) that quantify annual and seasonal differences in temperature, precipitation and moisture deficit across the species range. This yielded a total of 605 unique climate-associated SNPs from across the genome (Fig. 2D; Fig. S2-3), ranging from 74 to 154 SNPs associated with each climate variable. Populations entered the drought with different allele frequencies and genetic diversity at these loci, with southern populations harboring less standing variation at climate-associated loci despite having higher total genomic variation compared to northern populations (Fig. S4).

Next, to assess evidence for rapid evolution in response to exceptional drought, we tracked the changes in frequencies of climate-associated SNP through the drought by sequencing a "time series" dataset composed of 11 populations sampled annually between 2010 and 2016 (N= 401 individuals; Fig. 2B, Table S3). We tracked frequency change only for 374 SNPs that had a clear linear relationship with baseline climate (Supplemental Methods), to be able to set frequency = 1 as the drought-associated state for each SNP. For each SNP, we defined response to selection (S) as the slope of a generalized linear binomial model for SNP frequency over time (Fig. 2E; Fig. S5) (*11*). Since frequency = 1 is the drought-associated state of each SNP, a positive S indicates an increase in the frequency of drought-associated allele over time. This approach reveals extensive evidence of changes in frequencies of climate-associated SNPs across the range of *M. cardinalis* (Fig. 2E,F; Fig. S5-7). Median selection coefficients were significantly different from zero (the benchmark for no change) in 9 out of 11 populations (Table S4). Many climate-associated SNPs experienced weak positive selection (S=0 to 0.2), with a considerable number of SNPs showing moderate (S=0.2 to 0.5) or strong selection (S>0.5) towards the drought-associated state. Some SNPs also experienced negative selection, particularly in northern populations (Fig. 5-7). Nonetheless, even populations with negative median S values had dozens to hundreds of loci experiencing positive selection. Three out of the four most southern populations showed positive median selection values indicative of increases in the drought-associated allele, while four of seven central and northern populations showed median selection away from the direction predicted by SNP-environment associations (i.e., decreases in the drought-associated allele). Selection against alleles associated with historically hot and dry conditions could occur if these alleles encode (or are linked to loci that encode) trait values that promote drought escape in environments that favor alternative drought-response strategies such as avoidance or tolerance (*23, 24*). Consistent with this hypothesis, southern and northern populations differed in both the magnitude and direction of trait evolution in common gardens comparing anatomical, biochemical, and phenological traits of resurrected ancestors (families sampled pre-drought) and descendants (families sampled peak-drought) (*25*).

However, in addition to selection imposed directly or indirectly by the drought, genetic drift may also have driven allele frequency change, particularly because population sizes were small and usually declining during drought. To estimate the extent to which allele frequencies could be expected to change under drift alone, we created a null distribution of change in allele frequency by randomly selecting non-climate associated SNPs and calculating their slopes of change over time (Supplemental Methods). As expected under neutrality, null distributions of mean S for non-climate-associated SNPs were centred on zero (standard deviations ranged from +/-0.21 to +/-0.51

across populations). While all populations had positive selection for the drought-associated state in some SNPs, three populations had median selection strengths significantly greater than a null distribution of median selection strength from non-climate associated SNPs (Table S4, Fig. 2, Fig. S8; Sites 3, 4, 11). Two additional populations showed positive median selection, though these values were not significantly outside of the permuted null distribution of medians (Table S4, Fig. S8; Sites 2, 9). Non-random selection for alleles from historically hot and dry environments in southern California and the southern Sierra Nevada mountains corresponds with areas of consistently high drought severity during 2012-2015 (Fig. 1C), suggesting repeated instances of rapid evolution by natural selection due to exceptional drought.

So far we have demonstrated two parts of evolutionary rescue. *Mimulus cardinalis* populations were driven into decline by drought, and at least some rapidly evolved non-random increases in historically drought-associated alleles, though to different extents. To fully demonstrate evolutionary rescue, we must assess if populations recovered and if rapid evolution was responsible for this recovery. To test for recovery, we again used field demographic data on survival, growth, reproduction, and recruitment to infer $\boldsymbol{\lambda}$ via IPMs, this time using post-drought observations from the 2015-16 to the 2017-18 annual intervals, which is the relevant time window given life-history lags (*25*) (Supplemental Methods). Many *M. cardinalis* populations showed evidence of post-drought recovery (Fig. S1; Table S5), with mean growth rate above replacement ($\boldsymbol{\lambda}$>1) in 14 out of 19 populations. Still, there was much variability in the magnitude and stability of the recovery, with some populations showing a downward trajectory and three populations remaining locally extinct within our monitoring area (Fig. S1).

Post-drought population demography was strongly explained by response to selection at climate-associated loci during drought, providing evidence consistent with evolutionary rescue (Fig. 3). Among the subset of populations for which we had 2010-2016 timeseries genome sequences and suitable demographic recovery data (Table S2), greater rapid evolution, measured as greater median positive selection on the climate-associated SNPs, predicted greater mean population growth rates (Fig. 3C; P=0.019, R^2=0.46). This relationship is unaffected by two outliers (Table S6). Furthermore, nucleotide diversity of climate-associated SNPs prior to drought onset weakly predicted greater population recovery (Fig. 3D; P=0.093, R^2=0.12), although the majority of points showed an extremely tight relationship (P<0.0001, R^2=0.82 after removal of three outliers with outsized recruitment, a vital rate to which population growth estimates are highly sensitive). Critically, SNPs identified by GEA were necessary for explaining demographic recovery; genome-wide nucleotide diversity was uncorrelated with post-drought population growth rate (Fig. 3E; P=0.80, R^2<0.01) and showed no relationship with or without considering outliers (Table S6).

An alternative explanation for population recovery could be ecological rescue, where populations recovered simply because the drought ended. To assess ecological predictors of population recovery, we calculated post-drought climate anomalies as the deviations from 30-year pre-drought climate averages (1980-2010) for the means of each of eight precipitation and temperature-related variables during the recovery period (2015-17; Supplemental Methods). If demographic recovery is attributable simply to cessation of drought, then populations with wetter and cooler post-drought climate anomalies should have higher population growth rates. However, climate anomalies did not predict mean population growth rate following the drought across all 19 demography populations (Fig. 3F, Table S1). Another alternative explanation for population

183 recovery could be negative density-dependence, where the populations with the greatest decline
184 had greatest scope for recovery following the drought; however, we found no correlation between
185 mean lambda before vs. after drought (Fig. S9; r=0.01, P=0.98), which suggests population
186 recovery is not due to density-dependent demographic compensation. Further, it is improbable that
187 density-dependence could account for the relationships between post-drought population recovery
188 and genetic metrics (i.e., selection on, and standing nucleotide diversity of, climate-associated
189 SNPs). Thus, currently our best explanation for the observed variability in population recovery is
190 differences in capacity for evolutionary rescue.
191
192 Combining demographic and genomic data across space and time, we observed all three
193 requirements for evolutionary rescue in *M. cardinalis (4, 5)*. *Mimulus cardinalis* populations
194 declined during severe drought. Rapid evolution of drought-associated alleles occurred during this
195 population decline. Rapid evolution then predicted differences in demographic recovery.
196 Furthermore, populations harboring higher levels of nucleotide diversity at climate-associated
197 SNPs prior to the drought also had higher population recovery after drought, which implicates
198 adaptation from standing variation. Together these results show the importance of standing genetic
199 variation and evolution to drought resilience. Given the severe and far-reaching impacts of the
200 Western North American megadrought (*26-28*), significant pressure to rapidly evolve has likely
201 been widespread (*18, 29-31*). We have shown that evolutionary rescue is possible in a relatively
202 short-lived species (although longer-lived than most focal organisms in resurrection studies and
203 studies of evolutionary rescue) with high genetic variation, despite small census population sizes.
204 These results remain to be validated in species of conservation concern that may have much lower
205 genetic diversity and longer generation times. It is possible that evolutionary rescue, which we
206 have demonstrated here for *M. cardinalis*, could have also occurred in other short-lived species,
207 and might be critical for long-term population viability. Indeed, prior work on evolutionary rescue
208 in a microbial laboratory experiment suggests that populations and communities exposed to strong
209 but non-lethal stress may be better able to survive even more severe events in the future (*31, 32*).
210 Thus, populations of *M. cardinalis* and potentially other organisms may be better placed to survive
211 future climate extremes given the significant drought exposure. Alternatively, southern
212 populations might be nearing physiological limits (*33*) and selection might deplete genetic
213 variation and lessen future response to multivariate climate stressors.
214
215 The ability of genomics to predict future demographic outcomes is one of the most important open
216 questions within conservation genomics. There is considerable debate on the importance of
217 genome-wide diversity in conservation, where some studies find genome-wide diversity predictive
218 of population resilience (*34, 35*) while others find that direct information on adaptive genetic
219 variation is needed (*36, 37*). Moreover, validating the function and adaptive utility of GEA-
220 identified loci remains challenging (*38, 39*). Greater investigation into the ability of climate-
221 associated nucleotide diversity to predict demographic outcomes of systems undergoing climate
222 change may help assess broader utility of sequencing efforts for conservation management. Within
223 such efforts, we have shown that genotype-environment association is critical to identifying the
224 subset of genetic variation best able to predict demographic resilience to climate change when
225 clear climatic stressors are known (Fig. 3D vs. 3E). This provides a unique validation of GEA
226 inferences with independent demographic data, while lending support to the need to identify
227 adaptive loci within the genome. However, these GEA-identified SNP are not necessarily
228 indicative of the many other environmental stressors that populations will face. Thus, we

recommend using GEA-identified SNP sets, alongside genome-wide diversity approaches, when using nucleotide diversity to inform conservation management efforts for population resilience. These efforts could be used in conjunction with other spatially-based genetic diversity metrics such as the mutation-area relationship (*40*) and metrics of genomic maladaptation to climate change (*41, 42*) (*35, 36*). Ultimately, the idea that genetic variation spread across space can be used to predict genetic variation needed across time is a broadly used idea in evolutionary biology and conservation genetics (*38*). Our study supports the utility of space-for-time approaches in predicting real world eco-evolutionary outcomes.

References

1. H. O. Pörtner *et al.*, Climate change 2022: Impacts, Adaptation and Vulnerability. (2022).
2. IPCC, *Climate Change 2014: Impacts, Adaptation and Vulnerability: Regional Aspects*. (Cambridge University Press, Cambridge, United Kingdom and New York, NY, USA, 2014).
3. S. N. Sheth, A. L. Angert, Demographic compensation does not rescue populations at a trailing range edge. *Proceedings of the National Academy of Sciences* **115**, 2413-2418 (2018).
4. G. Bell, Evolutionary rescue. *Annual Review of Ecology, Evolution, and Systematics* **48**, 605-627 (2017).
5. R. Gomulkiewicz, R. D. Holt, When does evolution by natural selection prevent extinction? *Evolution* **49**, 201-207 (1995).
6. R. Gomulkiewicz, D. Houle, Demographic and genetic constraints on evolution. *The American Naturalist* **174**, E218-E229 (2009).
7. G. Bell, A. Gonzalez, Adaptation and evolutionary rescue in metapopulations experiencing environmental deterioration. *Science* **332**, 1327-1330 (2011).
8. A. Gonzalez, G. Bell, Evolutionary rescue and adaptation to abrupt environmental change depends upon the history of stress. *Philosophical Transactions of the Royal Society of London B: Biological Sciences* **368**, 20120079 (2013).
9. C. Costelloe, C. Metcalfe, A. Lovering, D. Mant, A. D. Hay, Effect of antibiotic prescribing in primary care on antimicrobial resistance in individual patients: systematic review and meta-analysis. *BMJ* **340**, (2010).
10. J. M. Kreiner, J. R. Stinchcombe, S. I. Wright, Population genomics of herbicide resistance: adaptation via evolutionary rescue. *Annual Review of Plant Biology* **69**, 611-635 (2018).
11. J. M. Kreiner *et al.*, Rapid weed adaptation and range expansion in response to agriculture over the past two centuries. *Science* **378**, 1079-1085 (2022).
12. B. Epstein *et al.*, Rapid evolutionary response to a transmissible cancer in Tasmanian devils. *Nature Communications* **7**, 1-7 (2016).
13. E. M. Oziolor *et al.*, Adaptive introgression enables evolutionary rescue from extreme environmental pollution. *Science* **364**, 455-457 (2019).
14. A. P. Williams, B. I. Cook, J. E. Smerdon, Rapid intensification of the emerging southwestern North American megadrought in 2020–2021. *Nature Climate Change* **12**, 232-234 (2022).
15. S. M. Robeson, Revisiting the recent California drought as an extreme value. *Geophysical Research Letters* **42**, 6771-6779 (2015).

16. J. Spinoni, G. Naumann, H. Carrao, P. Barbosa, J. Vogt, World drought frequency, duration, and severity for 1951–2010. *Internatonal Journal of Climatology.* **34**, 2792-2804 (2014).
17. C. D. Muir, A. L. Angert, Grow with the flow: a latitudinal cline in physiology is associated with more variable precipitation in *Erythranthe cardinalis*. *Journal of Evolutionary Biology* **30**, 2189-2203 (2017).
18. D. N. Anstett, H. A. Branch, A. L. Angert, Regional differences in rapid evolution during severe drought. *Evolution Letters*, (2021).
19. M. R. Easterling, S. P. Ellner, P. M. Dixon, Size-specific sensitivity: applying a new structured population model. *Ecology* **81**, 694-708 (2000).
20. M. Gautier, Genome-wide scan for adaptive divergence and association with population-specific covariates. *Genetics* **201**, 1555-1579 (2015).
21. T. R. Booker, S. Yeaman, J. R. Whiting, M. C. Whitlock, The WZA: a window-based method for characterizing genotype–environment associations. *Molecular Ecology Resources* **24**, e13768 (2024).
22. T. Wang, A. Hamann, D. Spittlehouse, C. Carroll, Locally downscaled and spatially customizable climate data for historical and future periods for North America. *PloS one* **11**, (2016).
23. N. J. Kooyers, The evolution of drought escape and avoidance in natural herbaceous populations. *Plant Science* **234**, 155-162 (2015).
24. F. Volaire, A unified framework of plant adaptive strategies to drought: Crossing scales and disciplines. *Global Change Biology* **24**, 2929-2938 (2018).
25. H. A. Branch, D. N. Anstett, A. L. Angert, Phenotypic lags influence rapid evolution throughout a drought cycle. *Evolution* **78**, 1067-1077 (2024).
26. C. Dong *et al.*, Vegetation responses to 2012–2016 drought in Northern and Southern California. *Geophysical Research Letters* **46**, 3810-3821 (2019).
27. M. J. Petrie *et al.*, Potential effects of drought on carrying capacity for wintering waterfowl in the Central Valley of California. *Journal of Fish and Wildlife Management* **7**, 408-422 (2016).
28. J. Lund, J. Medellin-Azuara, J. Durand, K. Stone, Lessons from California's 2012–2016 drought. *Journal of Water Resources Planning and Management* **144**, 04018067 (2018).
29. E. Hamann, A. E. Weis, S. J. Franks, Two decades of evolutionary changes in *Brassica rapa* in response to fluctuations in precipitation and severe drought. *Evolution* **72**, 2682-2696 (2018).
30. S. J. Franks, S. Sim, A. E. Weis, Rapid evolution of flowering time by an annual plant in response to a climate fluctuation. *Proceedings of the National Academy of Sciences* **104**, 1278-1282 (2007).
31. E. E. Dickman, L. K. Pennington, S. J. Franks, J. P. Sexton, Evidence for adaptive responses to historic drought across a native plant species range. *Evolutionary Applications* **12**, 1569-1582 (2019).
32. E. Low-Decarie *et al.*, Community rescue in experimental metacommunities. *Proceedings of the National Academy of Sciences,* **112**, 14307-14312 (2015).
33. H. A. Branch, D. R. Moxley, A. L. Angert, Regional differences in leaf evolution facilitate photosynthesis following severe drought. *New Phytologist* ***243***, 2457-2469 (2024).

34. M. Kardos *et al.*, The crucial role of genome-wide genetic variation in conservation. *Proceedings of the National Academy of Sciences* **118**, e2104642118 (2021).
35. S. Mathur, A. J. Mason, G. S. Bradburd, H. L. Gibbs, Functional genomic diversity is correlated with neutral genomic diversity in populations of an endangered rattlesnake. *Proceedings of the National Academy of Sciences* **120**, e2303043120 (2023).
36. Y. Willi *et al.*, Conservation genetics as a management tool: The five best-supported paradigms to assist the management of threatened species. *Proceedings of the National Academy of Sciences* **119**, e2105076119 (2022).
37. J. C. Teixeira, C. D. Huber, The inflated significance of neutral genetic diversity in conservation genetics. *Proceedings of the National Academy of Sciences* **118**, e2015096118 (2021).
38. R. S. Lovell, S. Collins, S. H. Martin, A. L. Pigot, A. B. Phillimore, Space-for-time substitutions in climate change ecology and evolution. *Biological Reviews* **98**, 2243-2270 (2023).
39. J. R. Lasky, E. B. Josephs, G. P. Morris, Genotype-environment associations to reveal the molecular basis of environmental adaptation. *Plant Cell* **35**, 125-138 (2023).
40. M. Exposito-Alonso *et al.*, Genetic diversity loss in the Anthropocene. *Science* **377**, 1431-1435 (2022).
41. C. Rellstab, B. Dauphin, M. Exposito-Alonso, Prospects and limitations of genomic offset in conservation management. *Evolutionary Applications*, (2021).
42. B. Dauphin *et al.*, Genomic vulnerability to rapid climate warming in a tree species with a long generation time. *Global Change Biology* **27**, 1181-1195 (2021).
43. D. N. Anstett, Anstett, J., Sheth, S. N., Moxley, D. R., Jahani, M., Huang, K., Todesco, M., Jordan, R., Lazaro-Guevara, J. M., Rieseberg, L. H., & Angert, A. L. anstettd/evol_rescue: Code for Evolutionary rescue during extreme drought. (Zenodo, 2024).
44. D. N. Anstett, Anstett, J., Sheth, S. N., Moxley, D. R., Jahani, M., Huang, K., Todesco, M., Jordan, R., Lazaro-Guevara, J. M., Rieseberg, L. H., & Angert, A. L. Supplemental files for Evolutionary rescue during extreme drought. (Zenodo, 2024).
45. W. L. Jepson, *The Jepson manual: higher plants of California*. (Univ of California Press, 1993).
46. J. L. Williams, T. E. Miller, S. P. Ellner, Avoiding unintentional eviction from integral projection models. *Ecology* **93**, 2008-2014 (2012).
47. S. N. A. Sheth, A. L. . (Dryad, 2019).
48. A. M. Bolger, M. Lohse, B. Usadel, Trimmomatic: a flexible trimmer for Illumina sequence data. *Bioinformatics* **30**, 2114-2120 (2014).
49. H. Li, R. Durbin, Fast and accurate short read alignment with Burrows–Wheeler transform. *Bioinformatics* **25**, 1754-1760 (2009).
50. P. Tools. (2020).
51. R. Poplin *et al.*, Scaling accurate genetic variant discovery to tens of thousands of samples. *BioRxiv*, 201178 (2017).
52. T. C. Nelson *et al.*, Quantitative trait locus mapping reveals an independent genetic basis for joint divergence in leaf function, life-history, and floral traits between scarlet monkeyflower (*Mimulus cardinalis*) populations. *American Journal of Botany* **108**, 844-856 (2021).

53. T. C. Nelson *et al.*, Ancient and recent introgression shape the evolutionary history of pollinator adaptation and speciation in a model monkeyflower radiation (*Mimulus* section Erythranthe). *PLoS Genetics* **17**, e1009095 (2021).
54. R Development Core Team, R: A language and environment for statistical computing. (2020).
55. J. Fox *et al.*, Package 'car'. *Vienna: R Foundation for Statistical Computing* **16**, (2012).
56. H. Wickham, ggplot2. *Wiley Interdisciplinary Reviews: Computational Statistics* **3**, 180-185 (2011).

Acknowledgements

J. Paul, A. Campbell-Craven, P. Beattie, J. Smith, A. Wilkinson, B. Econopouly, C. Fallon, E. Hinman, M. Bayly, D. Picklum, J. Perce, A. Agneray, M. Bontrager, M. Bayly, Q. Li, B. Gass, L. Super, E. Okun, T. Usui, R. Wilson, M. Nagaraj, and J. Wynne aided in demographic monitoring and seed collections. H. Branch, J. Zajonc, K. Saller, K. Beckett, and C. Longan aided in seed germination and greenhouse management. C. Elphinstone, and W. Cheng aided in DNA extractions and ordering. J. Whitton provided lab space and equipment. L. Fishman provided the *M. cardinalis* genetic map. S. Heredia provided illustration and figure design. Genome Quebec carried out library prep and Illumina Sequencing. Advance Research Computing at UBC provided computational resources and support. Special thanks to D. Lowry, W. Wetzel for advice and mentorship. Angert, Lowry and Wetzel labs provided feedback. **Funding:** This work was funded by a Genome BC Grant to A. Angert & L. Rieseberg; NSERC Banting, NSERC PDF, Killam Fellowship, and PRI Fellowship to D. Anstett; and NSERC Discovery grants to A. Angert and L. Rieseberg. S. Sheth was supported by NSF DEB-2131815 and USDA National Institute of Food and Agriculture Hatch 7002993. S. Sheth and A. Angert were supported by NSF DEB-2311414.
Authors contributions: D.N.A. led the project and was involved in all aspects. D.N.A., A.L.A, and L.H.R. conceived the project. R.J., S.N.S. and J.A. provided conceptual support. J.A. and D.N.A. performed bioinformatic and statistical analyses with support from M.J., K.H., J.M.L.G., R.J., A.L.A., and L.H.R.. A.L.A., S.N.S. and D.N.A. conducted demographic field work and seed collection. A.L.A. and S.N.S conducted demographic analyses. D.N.A., and A.L.A. curated seeds and generated leaf tissue for DNA extraction. D.R.M created the DNA extraction protocol. D.R.M & D.N.A conducted DNA extractions with support from M.T.. D.N.A., A.L.A., J.A., S.N.S, D.R.M. wrote the paper. All authors provided edits and feedback. **Competing interests:** Authors have no competing interests. **Data and materials availability:** All code is available on GitHub (https://github.com/anstettd/evol_rescue) and archived on Zenodo (43). SNP tables and additional supplemental files are also available on Zenodo (44). Raw reads have been deposited in the NCBI Sequence Read Archive under BioProject PRJNA1018529.

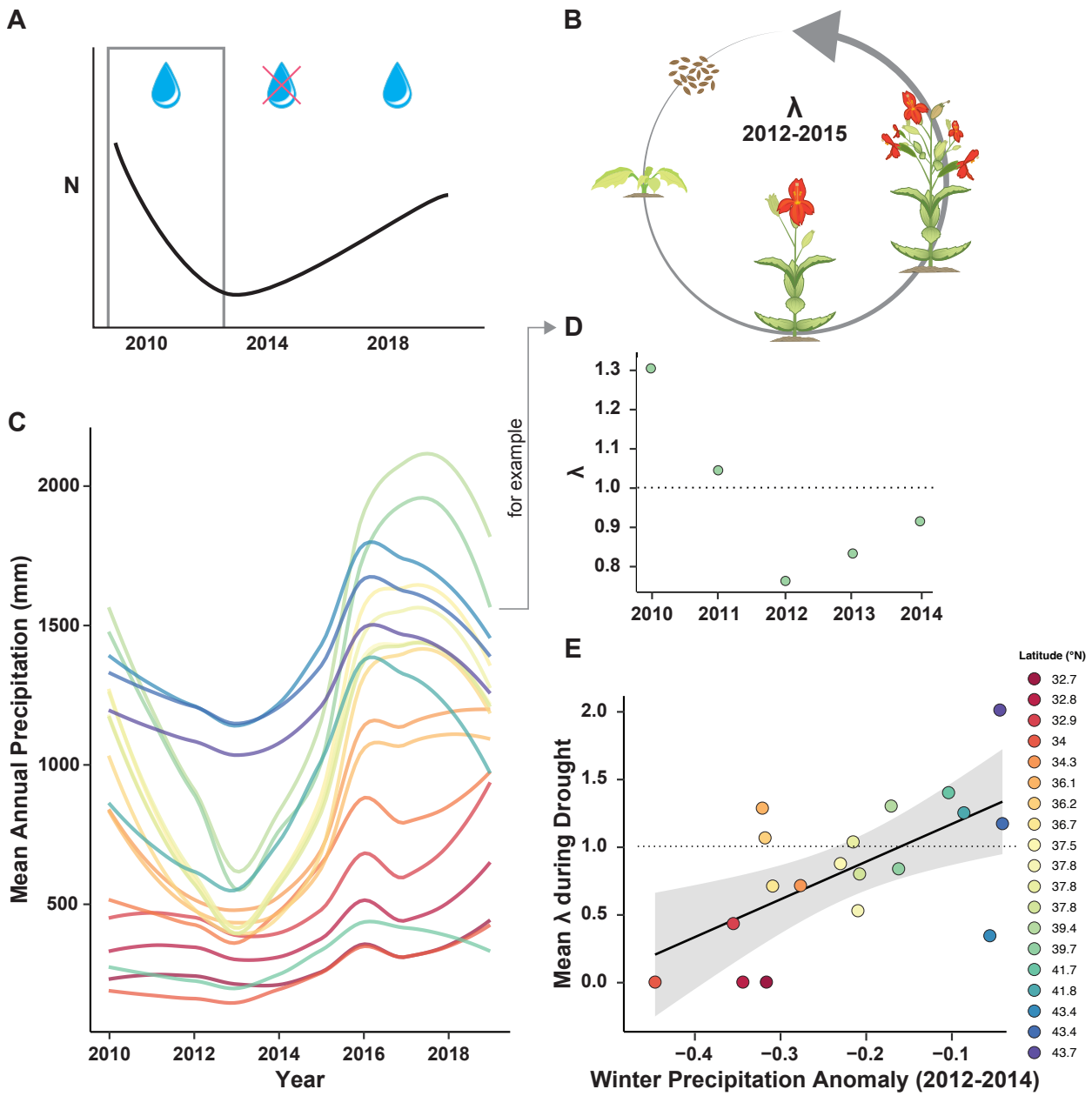

Fig. 1. Drought-induced demographic decline. (**A**) Decline phase of evolutionary rescue, indicated by a grey rectangle. (**B**) Demographic data observed from 2010 to 2015 are integrated into population growth estimates (***λ***) using integral projection models to quantify the extent of population decline. (**C**) Mean annual precipitation (mm) across 19 populations of *M. cardinalis* during record-setting drought and recovery. Each curve represents the precipitation time series for one population. Rainbow colouring indicates latitudinal position (red colors = lower latitudes, blue colors = higher latitudes). The green arrow indicates the population where demographic decline is further illustrated. (**D**) Example of the population along Little Jamison Creek (Plumas Eureka State Park, California, USA) where ***λ*** declined during drought-impacted years. Each dot gives one annual estimate from autumn of year *t* (indicated on x axis) to autumn of year *t*+1. The dashed black line depicts rate of replacement (***λ*** =1); values below this line indicate a population that is

projected to decline. (**E**) During severe drought, populations with greater precipitation anomalies (more negative values) experienced lower mean intrinsic growth rates during drought (P=0.005, R^2=0.35). Each point is one of the 19 populations where demography was assessed, colored by latitudinal position as in (**C**). The dashed line depicts rate of replacement ($\boldsymbol{\lambda}$ =1).

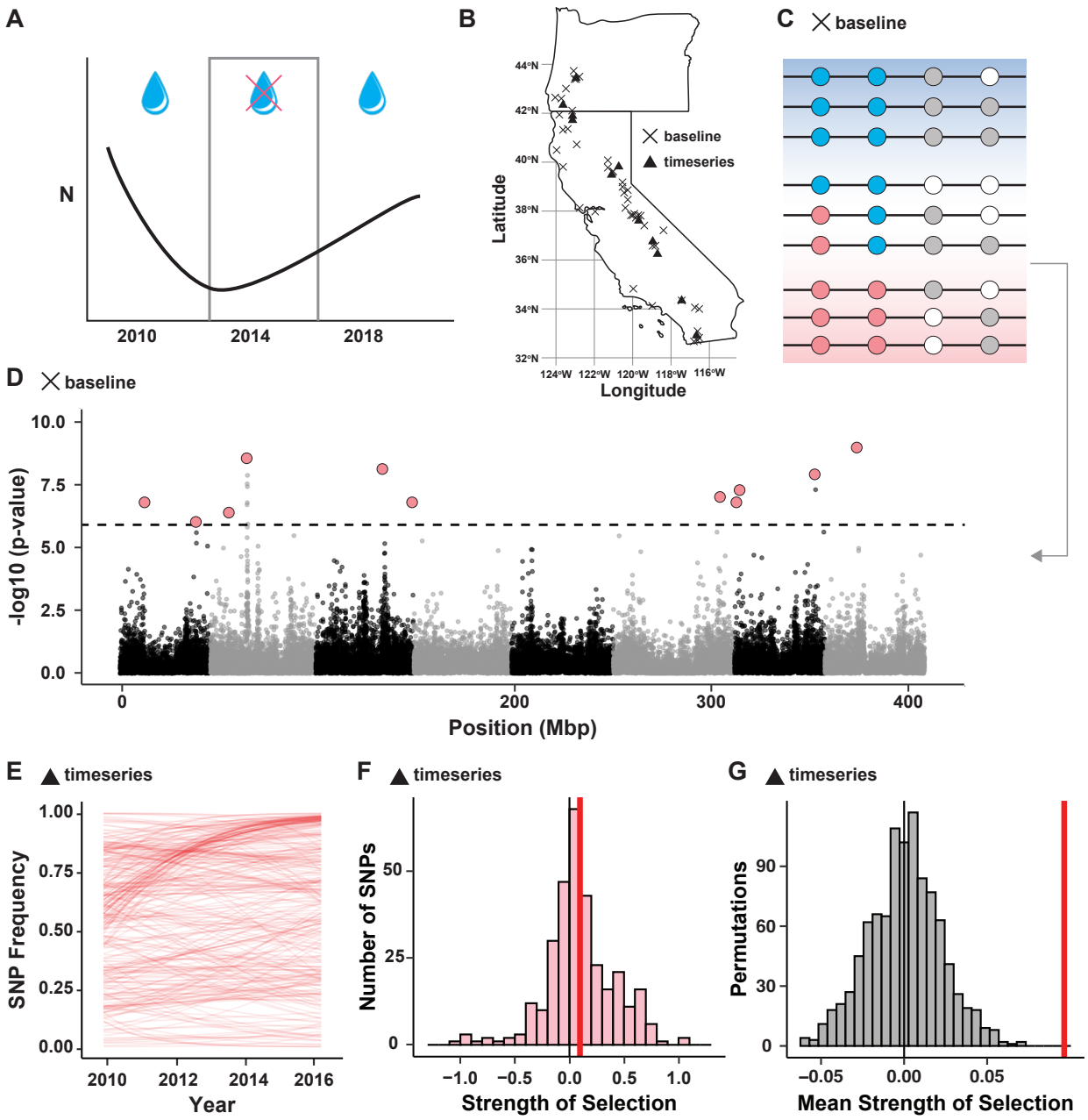

Fig 2. Rapid adaptation from standing genetic variation. Genotype-Environment Association (GEA) identifies Single Nucleotide Polymorphisms (SNPs) associated with spatial variation in historical climate, whose frequencies are then tracked over time during the (A) rapid evolution phase of evolutionary rescue, indicated by a grey rectangle. (B) Fifty-five "Baseline" *M. cardinalis* populations (X symbols) were sampled prior to record-setting drought (2007-2011) for GEA. Twelve "Time Series" populations (triangle symbols) were further sampled annually from 2010-2015, encompassing the extreme drought. (C) GEA on Baseline samples identifies SNPs associated with historical (1981-2010) spatial variation in temperature and precipitation. Cartoon depicts a climate gradient (cool and wet in blue to warm and dry in pink) with populations (horizontal lines) showing differences in the most prevalent SNP at four loci. Two climate-

associated loci (pink and blue alleles) and two non-climate associated loci (grey and white alleles) are shown. In this cartoon, SNP associated with warmer and drier conditions (pink alleles) are more prevalent in regions that have historically experienced more intense drought. These SNPs are putatively adaptive or physically close to putatively adaptive sites within the genome. (D) GEA of Baseline samples (X) reveals 10 Kbp windows associated with historic winter precipitation (1981 - 2010). Dashed line indicates the Bonferroni-corrected significance threshold. Pink dots represent peak 10-Kbp windows that were selected for further analyses (see Supplemental Methods for SNP set selection and Supplementary Results for all other climate variables). (E) Frequency changes over time, through extreme drought, for 374 climate-associated SNPs within Time Series samples (triangles) from a southern population (see Fig. S6 for all other populations). Each line represents a single regression (one per locus) whose slope is the response to selection (S). (F) Distribution of the strength of selection (S = slope of SNP change) across the climate-associated SNPs in Time Series samples (triangle) for this southern population. Histograms summarize the population of slopes depicted in panel E and give the number of observed SNPs within 0.1 S bins. Positive S indicates positive directional selection toward the heat/drought-associated allele identified during baseline GEA (i.e., pre-drought spatial associations of climate and SNP). The red vertical line gives the median S for this population. (G) Distribution of response to selection observed in 1000 permutations of non-climate associated SNP in Time Series samples (triangles) for the same southern population, shown as grey histograms. Median response to selection from climate-associated SNPs (red vertical line, as in E; note the difference in scale of x-axes) is compared to the median of the permuted distribution (grey vertical line). The observed response to selection at climate-associated SNP exceeds that of the random permutations in this population, suggesting that allele frequency change is driven by selection instead of drift.

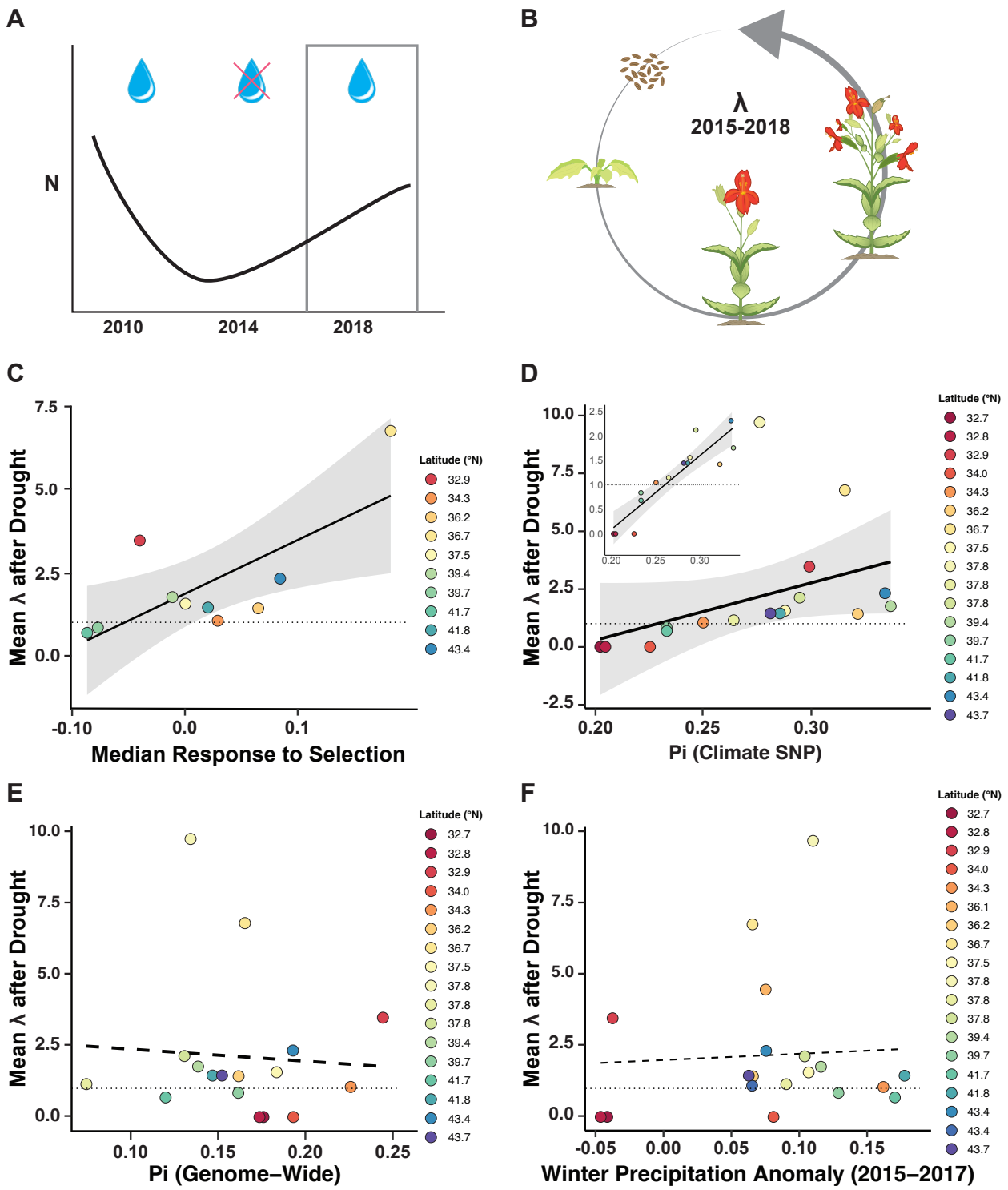

Fig 3. Rapid evolution and nucleotide diversity explain demographic recovery (A) Recovery phase of evolutionary rescue, indicated by a grey rectangle. (B) Demographic data observed from 2015 to 2018 are integrated into population growth estimates (***λ***) using IPM. (C) Greater median response to selection during severe drought predicts mean population growth rate during recovery. Each point represents one population, with only 10 populations having sufficient data for both

demographic estimates and time series genomics. (D) Greater nucleotide diversity (π) for climate-associated SNPs weakly predicts greater mean population growth rate. The majority of the data show an extreme tight correlation with climate-associated π (inset). 16 populations are included that have both baseline sequencing and demographic data. (E) Genome-wide nucleotide diversity (π) across all SNPs does not predict mean population growth rate. (F) Population recovery after severe drought (2015 to 2018) is not explained by less anomalous winter precipitation (or other climate variables; Table S1). Each point represents one population. The dashed line depicts rate of replacement ($\boldsymbol{\lambda}$ =1).